

# An unexpected cooling effect in Saturn's upper atmosphere

C. G. A. Smith<sup>1</sup>, A. D. Aylward<sup>1</sup>, G. H. Millward<sup>1</sup>†, S. Miller<sup>1</sup> & L. E. Moore<sup>2</sup>

**The upper atmospheres of the four Solar System giant planets exhibit high temperatures<sup>1,2</sup> that cannot be explained by the absorption of sunlight<sup>2,3</sup>. In the case of Saturn the temperatures predicted by models of solar heating<sup>2,4</sup> are ~200 K, compared to temperatures of ~400 K observed independently in the polar regions<sup>5</sup> and at 30° latitude<sup>6</sup>. This unexplained 'energy crisis' represents a major gap in our understanding of these planets' atmospheres. An important candidate for the source of the missing energy is the magnetosphere<sup>1,2,4,7–9</sup>, which injects energy mostly in the polar regions of the planet. This polar energy input is believed to be sufficient to explain the observed temperatures<sup>9</sup>, provided that it is efficiently redistributed globally by winds<sup>4,8</sup>, a process that is not well understood. Here we show, using a numerical model<sup>4</sup>, that the net effect of the winds driven by the polar energy inputs is not to heat but to cool the low-latitude thermosphere. This surprising result allows us to rule out known polar energy inputs as the solution to the energy crisis at Saturn. There is either an unknown—and large—source of polar energy, or, more probably, some other process heats low latitudes directly.**

Recent numerical modelling studies<sup>4,8</sup> have shown that under specific circumstances polar energy inputs may explain the high thermospheric temperatures at Saturn. For plausible heating distributions in the polar regions there is predicted to exist a system of equatorward winds that redistribute the energy globally, generating the observed temperatures at both low and high latitudes. But these studies consider only the effects of pure thermal energy inputs on the thermosphere, whereas the bulk of the polar energy input from the magnetosphere is thought to be a mixture of thermal energy (Joule heating) and kinetic energy (ion drag) in roughly equal proportions<sup>7,9</sup>. The kinetic energy input is necessarily accompanied by an input of angular momentum. The sense of this angular momentum input is westward, that is, in the opposite direction to that of the planetary rotation. The overall effect of ion drag on the dynamics is thus expected to be the generation of strong westward winds throughout the polar thermosphere. Here we address for the first time to our knowledge the effect of these westward winds on the structure of the thermosphere.

We use a numerical thermosphere model<sup>4</sup> based on a widely used model of the terrestrial thermosphere<sup>10</sup>, converted to an atmosphere composed of H<sub>2</sub>, H and He. It uses an eulerian grid on which temperatures and the three components of the neutral wind are calculated by time integration. The lower boundary is placed at an altitude of 800 km above the 1 bar level, and at a fixed pressure of 100 nbar. At this level we assume a fixed temperature of 143 K (ref. 11) and a horizontal wind velocity of zero. We parameterize the vertical transport of energy and momentum by small-scale motions using an eddy diffusion coefficient<sup>12</sup> of  $K_z = 10^4 \text{ m}^2 \text{ s}^{-1}$ . For this study, we simplify the model by assuming that the system is symmetric about the

planet's axis of rotation and mirror-symmetric about the equatorial plane. These are good approximations because Saturn's magnetic field almost exhibits both of these symmetries<sup>13</sup>. Furthermore, the dynamics of the magnetosphere are strongly dominated by the planetary rotation and can be approximated as axially symmetric to first order<sup>9</sup>. We expect deviations from our assumed symmetries to be second-order effects. We note that the introduction of axial symmetry does not mean that we do not model zonal (east–west) winds: the effects of zonal winds are fully included in the model, but they are assumed to be identical at all longitudes. The introduction of these symmetry assumptions allows us to use very high grid resolutions in our model. We employ a latitudinal resolution of 0.2° and a vertical resolution of 0.2 pressure scale heights. Further details and discussion of the model are given in the Supplementary Methods.

This basic model is forced only by solar heating. Running this model to near steady state (requiring a run time of 400 planetary rotations<sup>8</sup>) predicts roughly uniform global temperatures of ~150–160 K (Supplementary Fig. 1), with the higher temperatures at the equator. To include the polar energy inputs, we require models of the ionospheric conductivity and plasma flows. Good empirical models of the ionospheric conductivity do not exist, owing to lack of data. For this reason we use a conductivity distribution calculated using a numerical model of the ionosphere<sup>14</sup>. We use ion and electron densities from this model to calculate a global distribution of conductivity and fix these values with respect to our thermosphere model. The ionospheric plasma flows are taken from an empirical model<sup>9</sup> based on a mixture of *in situ* spacecraft<sup>15</sup> and ground-based spectroscopic data<sup>16</sup>. This model predicts that the magnetosphere will exert a westward ion drag on the thermosphere poleward of ~65° latitude. Thus we expect the Joule heating and ion drag to be significant only in this region. Further details of both these models, and our formulation of Joule heating and ion drag, are given in the Supplementary Methods.

Including these inputs in the model generates the structures shown in Fig. 1. Comparing this run to the control run forced only by solar heating shows that Joule heating and ion drag cause net heating poleward of and net cooling equatorward of the dashed line. The maximum cooling effect is ~7 K at ~65° latitude. Although small, this effect is unexpected, counter-intuitive and rather surprising. It can be explained by inspecting the meridional circulation, which shows a poleward flow at low altitudes and an equatorward flow at high altitudes. The low-altitude flow is energetically the more important because the density of the atmosphere decreases with increasing altitude. Thus the dynamical coupling between low and high latitudes is dominated by a steady flow of gas—and therefore energy—away from low latitudes and into the polar regions. This acts both to enhance convective cooling of low latitudes, and to heat the polar region. The flows themselves arise because of small force imbalances in the thermosphere. In Fig. 2 we show a conceptual

<sup>1</sup>Department of Physics and Astronomy, University College London, WC1E 6BT, UK. <sup>2</sup>Center for Space Physics, Boston University, Boston, Massachusetts 02215, USA. †Present address: Laboratory for Atmospheric and Space Physics, University of Colorado, Boulder, Colorado 80303, USA.

interpretation of these flows in terms of the hydrostatic balance in the upper atmosphere; in the Supplementary Discussion we also present an analysis of the actual forces calculated by the model.

It is clear from Fig. 1 that, while our model does reproduce the observed temperature of  $\sim 400$  K in the polar regions<sup>5</sup>, we do not reproduce the observed value of  $\sim 400$  K at  $30^\circ$  latitude<sup>6</sup>, because we predict cooling everywhere equatorward of  $55^\circ$  latitude. The initial indication is thus that the polar energy inputs resolve the high-latitude

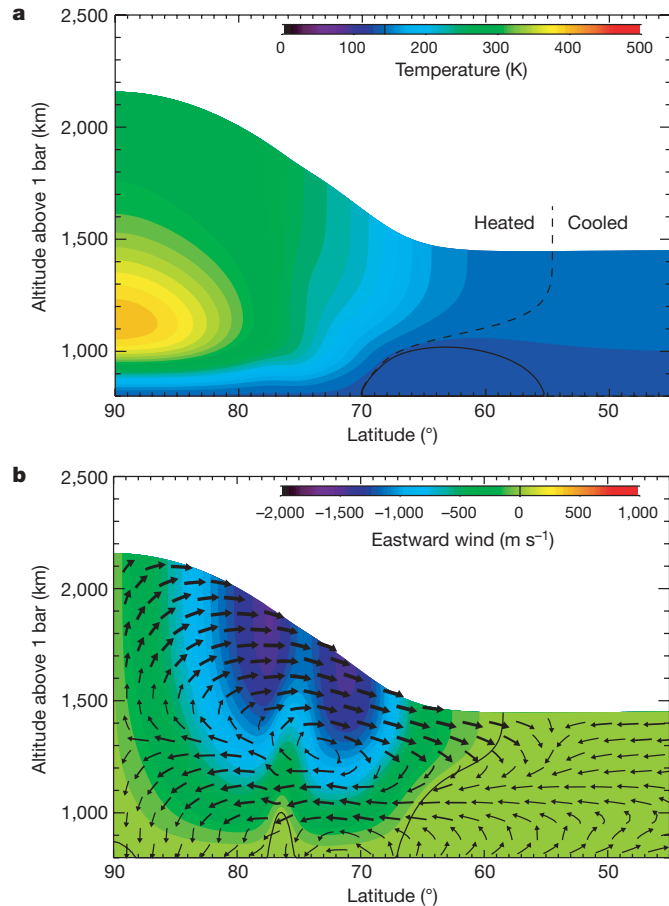


**Figure 1 | Thermal and dynamical structure of the upper atmosphere predicted by our model.** **a**, Temperature structure (colour contours). The dashed line separates regions to the left, which are heated by the polar energy inputs, from regions on the right, which are cooled. At latitudes smaller than those shown the temperature profile remains approximately constant to the equator, exhibiting exospheric temperatures of 150–160 K. It is thus clear that the polar energy inputs do not reproduce the observed temperature of  $\sim 400$  K at  $30^\circ$  latitude<sup>6</sup>. However, the temperature of  $\sim 400$  K at the pole is a good match to the infrared spectroscopic temperatures determined in this region<sup>5</sup>. The solid contour represents the fixed lower-boundary temperature of 143 K. The region enclosed by this contour at  $\sim 55$ – $70^\circ$  latitude is thus cooler than the lower-boundary temperature. **b**, Zonal winds (colour contours). The zero contour of zonal wind is shown by the solid line. Poleward of  $\sim 65^\circ$  latitude the winds are almost entirely westward, as expected from the direction of ion drag. The double-lobed structure in the zonal winds is due to structures in the plasma flow model (see the Supplementary Information). Arrows show the combined vertical and meridional circulation. The thinnest arrows represent wind speeds of  $<1$  m s<sup>-1</sup>, the thickness increasing linearly with the logarithm of wind speed until the thickest arrows represent wind speeds of  $>100$  m s<sup>-1</sup>. The cooling effect is produced by two mechanisms. First, the poleward flow induced by ion drag enhances the convective cooling of the low-latitude regions. Second, the increase in the poleward wind speed between  $55^\circ$  and  $70^\circ$  latitude represents a divergence in the flow that must be balanced by upwelling to satisfy continuity. This upwelling gas expands, and cools adiabatically. It is this effect that produces temperatures cooler than the lower-boundary temperature in this region.

400

energy crisis but do not resolve the low-latitude energy crisis. However, we must consider whether our results depend on our choice of model inputs. The input in which we have the least confidence is the ionospheric conductivity model: while our thermospheric boundary conditions and plasma flow model are well supported by the available data, the conductivity model is not. In particular, the model currently only includes ionization due to absorption of solar radiation, and so it most probably underestimates the conductivity in the polar regions, where particle precipitation is an important source of ionization. We have thus performed a sensitivity study in which we artificially scale up the conductivity globally by fixed factors. The effect of this alteration is simply to intensify the behaviour described above. If the scaling factor is 16, the polar hot-spot reaches temperatures greater than 500 K and the maximum degree of cooling compared to the control run increases to  $\sim 27$  K (see the Supplementary Discussion for further details). Thus we still approximately match the observed high-latitude temperature and still fail to match the observed low-latitude temperature.

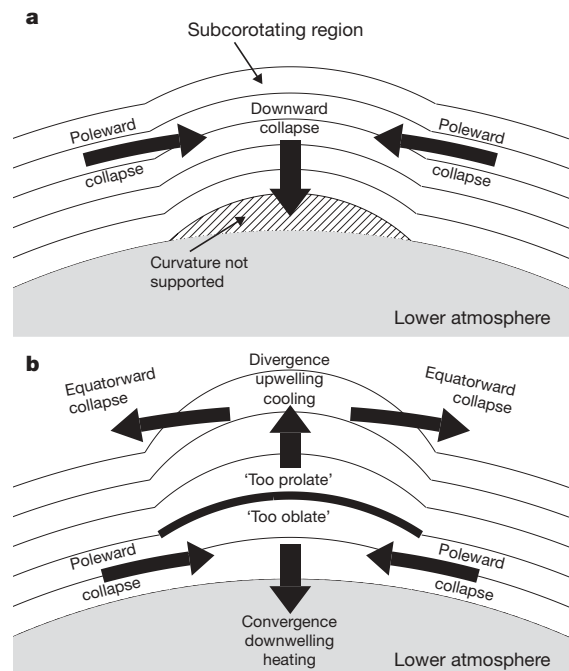


**Figure 2 | Interpretation of polar dynamics in terms of hydrostatic balance.**

For the atmosphere to rest in hydrostatic balance, we require internal pressure gradients to perfectly balance the combined gravitational and centrifugal accelerations. For this reason, surfaces of constant pressure normally align themselves with surfaces of constant potential energy: this is the cause of Saturn's considerable oblateness. If the polar upper atmosphere is made to rotate more slowly by ion drag, but in the same gravity field, it must adopt a less-oblate profile if it is to rest in perfect hydrostatic balance. In **a**, we show the situation that this implies if the atmosphere is isothermal. Here the grey shaded region represents the atmosphere lying below the region that we model and the solid lines represent surfaces of constant pressure in the upper atmosphere. In the subcorotating region close to the pole, the less-oblate profile that we require is not supported by the lower atmosphere, and the gas thus 'collapses' towards the pole and downwards. This inward flow is strongly convergent, causing downwelling and compression that heats the gas. The steady-state situation is sketched in **b**. Here, the compressional heating at the pole has increased the scale height, allowing a less-oblate profile to be supported. However, owing to the efficiency of vertical thermal conduction, this increased scale height persists at all altitudes. Thus, there is a particular pressure surface for which the curvature is 'just right' to support the rotation velocity of the gas (thick line). At lower altitudes the curvature is 'too oblate' to support the rotation, and the gas continues to collapse inwards and provide compressional heating. At higher altitudes the curvature is 'too prolate' and the gas collapses away from the pole.

We must also ask whether we are omitting any important sources of polar energy. The only well-quantified source of polar energy other than those used in our model is energy deposition by the particle precipitation that forms the ultraviolet aurora<sup>9,17</sup>. This has already been shown to have a negligible effect on the thermal structure<sup>8</sup>. It has also been suggested that small-scale structures in the ionospheric plasma flow may greatly increase the total Joule heating<sup>7,18</sup> without a corresponding increase in ion drag. Such structures would presumably originate in the magnetosphere and solar wind. Data collected in these regions by the Cassini mission may allow quantification of this small-scale structure and its implications for the flow of energy within the magnetosphere–atmosphere system.

However, the good match between our results and the high-latitude temperature measurements<sup>5</sup> suggests that if we were to introduce additional polar energy inputs that were sufficient to outweigh the cooling effect and thus resolve the low-latitude energy crisis, we would probably overheat the polar regions. Thus our results strongly suggest that low latitudes are heated directly, perhaps by the breaking of buoyancy waves generated in the lower atmosphere<sup>19–22</sup>. There may also be some Joule heating or particle precipitation at low latitudes that has yet to be accounted for. The Cassini mission may contribute to an improved understanding of such processes by providing new measurements of the thermospheric temperature. Although a number of low-latitude temperature measurements are at present available, they are neither mutually consistent nor unambiguous<sup>6,23–25</sup>. A multi-latitude thermospheric data set collected by Cassini and analysed self-consistently would thus be an invaluable resource.

In summary, our conclusions indicate strongly that polar energy inputs are not the solution to the low-latitude energy crisis at Saturn, and that future research should thus focus on direct heating of low latitudes. We expect our results to apply in outline to the slightly more complicated situation at Jupiter, and preliminary results from a jovian version of our model support this prediction. However, we are not yet in a position to assess whether our cooling effect may be relevant to the energy crises at Uranus and Neptune, given the apparent complexity of their magnetospheres, but this study does indicate that magnetosphere–atmosphere coupling at these planets is likely to be complicated and may throw up further surprises.

Received 11 July; accepted 8 December 2006.

1. Atreya, S. K. *Atmosphere and Ionospheres of the Outer Planets and their Satellites* Ch. 2 (Springer, Heidelberg, 1986).
2. Yelle, R. V. & Miller, S. in *Jupiter: Planet, Satellites and Magnetosphere* (eds Bagenal, F., McKinnon, W. & Dowling, T.) 185–218 (Cambridge Univ. Press, Cambridge, UK, 2004).
3. Strobel, D. F. & Smith, G. R. On the temperature of the jovian thermosphere. *J. Atmos. Sci.* **30**, 718–725 (1973).
4. Mueller-Wodarg, I. C. F., Mendillo, M., Yelle, R. V. & Aylward, A. D. A global circulation model of Saturn's thermosphere. *Icarus* **180**, 147–160 (2006).
5. Melin, H. *Comparative Aeronomy of the Upper Atmospheres of the Giant Planets*. PhD thesis, Univ. London (2006).

6. Smith, G. R. *et al.* Saturn's upper atmosphere from the Voyager 2 EUV solar and stellar occultations. *J. Geophys. Res.* **88**, 8667–8679 (1983).
7. Smith, C. G. A., Miller, S. & Aylward, A. D. Magnetospheric energy inputs into the upper atmospheres of the giant planets. *Ann. Geophys.* **23**, 1943–1947 (2005).
8. Smith, C. G. A., Aylward, A. D., Miller, S. & Mueller-Wodarg, I. C. F. Polar heating in Saturn's thermosphere. *Ann. Geophys.* **23**, 2465–2477 (2005).
9. Cowley, S. W. H., Bunce, E. J. & O'Rourke, J. M. A simple quantitative model of plasma flows and currents in Saturn's polar ionosphere. *J. Geophys. Res.* **A18**, 5212–5230 (2004).
10. Fuller-Rowell, T. J. *et al.* in *STEP Handbook of Ionospheric Models* 217–238 (SCOSTEP, Logan, Utah, 1996).
11. Moses, J. I. *et al.* Photochemistry of Saturn's atmosphere. I. Hydrocarbon chemistry and comparisons with ISO observations. *Icarus* **143**, 244–298 (2000).
12. Atreya, S. K. Eddy mixing coefficient on Saturn. *Planet. Space Sci.* **30**, 849–854 (1982).
13. Davis, L. J. & Smith, E. J. A model of Saturn's magnetic field based on all available data. *J. Geophys. Res.* **95**, 15257–15261 (1990).
14. Moore, L. E., Mendillo, M., Mueller-Wodarg, I. C. F. & Murr, D. L. Modeling of global variations and ring shadowing in Saturn's ionosphere. *Icarus* **172**, 503–520 (2004).
15. Richardson, J. D. Thermal ions and Saturn—Plasma parameters and implications. *J. Geophys. Res.* **91**, 1381–1389 (1986).
16. Stallard, T. S., Miller, S., Trafton, L. M., Geballe, T. R. & Joseph, R. D. Ion winds in Saturn's southern auroral/polar region. *Icarus* **167**, 204–211 (2004).
17. Clarke, J. T. *et al.* Morphological differences between Saturn's ultraviolet aurorae and those of Earth and Jupiter. *Nature* **433**, 717–719 (2005).
18. Codrescu, M. V., Fuller-Rowell, T. J. & Foster, J. C. On the importance of E-field variability for Joule heating in the high-latitude thermosphere. *Geophys. Res. Lett.* **22**, 2393–2396 (1995).
19. Young, L. A., Yelle, R. V., Young, R., Seiff, A. & Kirk, D. B. Gravity waves in Jupiter's thermosphere. *Science* **276**, 108–111 (1997).
20. Matcheva, K. I. & Strobel, D. F. Heating of Jupiter's thermosphere by dissipation of gravity waves due to molecular viscosity and heat conduction. *Icarus* **140**, 328–340 (1999).
21. Hickey, M. P., Walterscheid, R. L. & Schubert, G. Gravity wave heating and cooling in Jupiter's thermosphere. *Icarus* **148**, 266–281 (2000).
22. Hickey, M. P., Schubert, G. & Walterscheid, R. L. Gravity wave heating and cooling in Saturn's thermosphere. *Eos* **86** (Suppl. 18), abstr. SA24A–06 (2005).
23. Festou, M. C. & Atreya, S. K. Voyager ultraviolet stellar occultation measurements of the composition and thermal profiles of the Saturnian upper atmosphere. *Geophys. Res. Lett.* **9**, 1147–1150 (1982).
24. Atreya, S. K., Waite, J. H., Donahue, T. M., Nagy, A. F. & McConnell, J. C. in *Saturn* (eds Gehrels, T. & Matthews, M. S.) 239–277 (Univ. Arizona Press, Tucson, Arizona, 1984).
25. Smith, G. R. & Hunten, D. M. Study of planetary atmospheres by absorptive occultations. *Rev. Geophys.* **28**, 117–143 (1990).

**Supplementary Information** is linked to the online version of the paper at [www.nature.com/nature](http://www.nature.com/nature).

**Acknowledgements** The simulations described in this study were performed using the HiPerSPACE facility at UCL, funded by the UK Particle Physics and Astronomy Research Council (PPARC). C.G.A.S. acknowledges receipt of a CASE studentship funded by PPARC and Sun Microsystems Ltd.

**Author Contributions** The thermosphere modelling was carried out by C.G.A.S., A.D.A., G.H.M. and S.M. L.E.M. provided the ionosphere model.

**Author Information** Reprints and permissions information is available at [www.nature.com/reprints](http://www.nature.com/reprints). The authors declare no competing financial interests. Correspondence and requests for materials should be addressed to A.D.A. ([a.aylward@ucl.ac.uk](mailto:a.aylward@ucl.ac.uk)).